

1 Ancestry process for infectious disease outbreaks with superspreading

2 Xavier Didelot^{1,2,*}, Ian Roberts², ...

3 ¹ School of Life Sciences, University of Warwick, United Kingdom

4

5 ² Department of Statistics, University of Warwick, United Kingdom

6

7 * Corresponding author. Tel: 0044 (0)2476 572827. Email: `xavier.didelot@gmail.com`

8 Running title: Ancestry for outbreaks with superspreading

9 Keywords: infectious disease epidemiology modelling; offspring distribution; superspreading;
10 outbreaks; lambda-coalescent model; multiple mergers

1 Introduction

An outbreak of an infectious disease typically starts when a single or a small number of infected individuals appear within a susceptible population. Each infected individual may come in contact and infect each of the susceptible individuals, who will then become infected in their turn and spread the disease further. Most infectious disease modelling theory describes situations where the disease is at an equilibrium, when the number of infected individuals is high and/or with a significant part of the population already infected (Anderson and May 1991; Keeling and Rohani 2008). Here however we focus on the early stages of an epidemic, where the number of infected individuals is small and the number of susceptibles relatively high and unchanging. In this situation it is useful to think about the number of infections that each newly infected individual is likely to cause, and the probabilistic distribution for this number is often called the offspring distribution (Grassly and Fraser 2008). The mean of the offspring distribution is called the basic reproduction number R_0 and has been given much attention especially since it determines how likely the outbreak is to spread, and how much effort would be needed to bring it under control (Fraser et al. 2004).

If we consider that all individuals are infectious for the same duration and with the same infectiousness, the offspring distribution is Poisson distributed with mean R_0 , which means that the variance of the offspring distribution is also R_0 . We would then say that there is no transmission heterogeneity. However, in practice there are many reasons why this may not be the case, with some individuals being infectious for longer, or being more infectious than others, or having more contacts with susceptibles, or being less symptomatic and therefore less likely to reduce contact numbers, etc. All these factors cause the offspring distribution to be more dispersed than it would otherwise be, that is to have a variance greater than its mean R_0 . A frequent choice to capture this overdispersion is to model the offspring distribution using a Negative-Binomial distribution with mean R_0 and dispersion parameter r (Lloyd-Smith et al. 2005; Grassly and Fraser 2008). When r is close to zero the variance is high compared to the mean, whereas when r is high the variance becomes close to the mean. This transmission heterogeneity is often called superspreading, although this is perhaps misleading as it is the rule rather than the exception of how infectious diseases spread. Superspreading has indeed been described in many diseases (Woolhouse et al. 1997; Stein 2011; Wang et al. 2021), and most recently for SARS-CoV-2 (Wang et al. 2020; Lemieux et al. 2021; Gómez-Carballa et al. 2021).

As an outbreak unfolds forward-in-time, a transmission tree is generated representing who-infected-whom, in which each node is an infected individual and points towards a number of nodes distributed according to the offspring distribution. Here we consider the reverse problem of the transmission ancestry, going backward-in-time, of a sample of infected individuals.

2 General case

Let time be measured in discrete units and denoted t . Each discrete value of t correspond to a unique non-overlapping generations of infected individuals, so that individuals infected at t will have offspring at $t + 1$, etc. Let N_t denote the number of infectious individuals at time t . Each of them creates a number $s_{t,i}$ of secondary infections at time $t + 1$, following the offspring distribution $\alpha_t(s)$. The mean of this distribution is the basic reproduction number R_t and the variance is V_t . We have:

$$N_{t+1} = \sum_{i=1}^{N_t} s_{t,i} \quad (1)$$

2.1 Inclusive coalescence probability

We define the inclusive coalescence probability $p_{k,t}(N_t, N_{t+1})$ as the probability that a specific set of k individuals from generation $t+1$ find a common ancestor in generation t , conditional on population sizes N_t and N_{t+1} .

Given full information about offspring counts from individuals in generation t , $\mathbf{s}_t = (s_{t,1}, \dots, s_{t,N_t})$, we have

$$\begin{aligned} p_{k,t}(\mathbf{s}_t, N_t) &= \sum_{i=1}^{N_t} \frac{\binom{s_{t,i}}{k}}{\binom{N_{t+1}}{k}} \\ &= \sum_{i=1}^{N_t} \frac{\Gamma(s_{t,i} + 1) \Gamma(N_{t+1} - k + 1)}{\Gamma(s_{t,i} - k + 1) \Gamma(N_{t+1})}. \end{aligned} \quad (2)$$

Full information $\{s_{t,i}\}$ yields the population size N_{t+1} but is not feasible to observe in practice. We can instead express the inclusive coalescence probability conditioning on the next population size N_{t+1} by summing over possible offspring counts $\mathbf{s}_t = (s_{t,1}, \dots, s_{t,N_t})$ conditional on the total generation size. Let $S_t^{-(1)} = (S_{t,2}, \dots, S_{t,N_t})$.

$$\begin{aligned} p_{k,t}(N_t, N_{t+1}) &= \sum_{\mathbf{s}_t \in \mathbb{N}_0^{N_t}} \mathbb{P} \left[\mathbf{S}_t = \mathbf{s}_t \mid \sum_{i=1}^{N_t} S_{t,i} = N_{t+1} \right] p_{k,t}(\mathbf{s}_t, N_t) \\ &= \sum_{\mathbf{s}_t \in \mathbb{N}_0^{N_t}} \mathbb{P} \left[\mathbf{S}_t = \mathbf{s}_t \mid \sum_{i=1}^{N_t} S_{t,i} = N_{t+1} \right] \sum_{i=1}^{N_t} \frac{\binom{s_{t,i}}{k}}{\binom{N_{t+1}}{k}} \\ &= \sum_{i=1}^{N_t} \sum_{\mathbf{s}_t \in \mathbb{N}_0^{N_t}} \frac{\binom{s_{t,i}}{k}}{\binom{N_{t+1}}{k}} \mathbb{P} \left[S_{t,1} = s_{t,1}, \mathbf{S}_t^{-(1)} = \mathbf{s}_t^{-(1)} \mid \sum_{i=1}^{N_t} S_{t,i} = N_{t+1} \right] \\ &= \frac{N_t}{\binom{N_{t+1}}{k}} \sum_{\mathbf{s}_t \in \mathbb{N}_0^{N_t}} \binom{s_{t,1}}{k} \mathbb{P} \left[S_{t,1} = s_{t,1} \mid \sum_{i=1}^{N_t} S_{t,i} = N_{t+1} \right] \\ &\quad \times \mathbb{P} \left[\mathbf{S}_t^{-(1)} = \mathbf{s}_t^{-(1)} \mid S_{t,1} = s_{t,1}, \sum_{i=1}^{N_t} S_{t,i} = N_{t+1} \right] \\ &= \frac{N_t}{\binom{N_{t+1}}{k}} \sum_{s_{t,1}=0}^{N_{t+1}} \binom{s_{t,1}}{k} \mathbb{P} \left[S_{t,1} = s_{t,1} \mid \sum_{i=1}^{N_t} S_{t,i} = N_{t+1} \right] \end{aligned}$$

$$\begin{aligned}
& \times \underbrace{\sum_{\mathbf{s}_t^{-(1)} \in \mathbb{N}_0^{N_t-1}} \mathbb{P} \left[\mathbf{s}_t^{-(1)} = \mathbf{s}_t^{-(1)} \middle| \sum_{i=2}^{N_t} S_{t,i} = N_{t+1} - s_{1,t} \right]}_{=1} \\
& = \frac{N_t}{\binom{N_{t+1}}{k}} \mathbb{E} \left[\binom{S_{t,1}}{k} \middle| \sum_{i=1}^{N_t} S_{t,i} = N_{t+1} \right] \tag{3}
\end{aligned}$$

61

62 The falling factorial moments $\mathbb{E} \left[\frac{S_{t,1}!}{(S_{t,1}-k)!} \middle| \sum_{i=1}^{N_t} S_{t,i} = N_{t+1} \right]$ in Equation (3) can be readily obtained
63 by differentiating the probability generating function of $S_{t,1} | (\sum_{i=1}^{N_t} S_{t,i} = N_{t+1})$.

64 2.2 Exclusive coalescence probability

65 Generally, we observe a sample of individuals from each generation rather than the entire population.
66 In this case, we are interested in the exclusive coalescence probability $p_{n,k,t}(N_t, N_{t+1})$ that exactly k
67 individuals from a sample of n arose from a common ancestor one generation in the past given knowlege
68 of the total population sizes N_t and N_{t+1} .

69 Given full information about offspring counts of the parents of sampled individuals at the present,
70 $\mathbf{x}_t = (x_{t,1}, \dots, x_{t,N_t})$, we have

$$\begin{aligned}
p_{n,k,t}(\mathbf{x}_t, N_t) &= \sum_{i=1}^{N_t} \frac{\binom{x_{t,i}}{k}}{\binom{n}{k}} \mathbb{I}\{x_{t,i} = k\} \\
&= \sum_{i=1}^{N_t} \frac{x_{t,i}!}{(x_{t,i} - k)!} \frac{(n - k)!}{n!} \mathbb{I}\{x_{t,i} = k\}. \tag{4}
\end{aligned}$$

71 Similarly to the exclusive coalescence probability, we can use this to evaluate the exclusive probability
72 given N_t and N_{t+1} by summing over possible parent offspring configurations (for $k \leq n$),

$$\begin{aligned}
p_{n,k,t}(N_t, N_{t+1}) &= \sum_{\mathbf{x}_t \in \mathbb{N}_0^{N_t}} \mathbb{P} \left[\mathbf{X}_t = \mathbf{x}_t \middle| \sum_{i=1}^n X_{t,i} = n \right] p_{n,k,t}(\mathbf{x}_t, N_t) \\
&= \sum_{\mathbf{x}_t \in \mathbb{N}_0^{N_t}} \mathbb{P} \left[\mathbf{X}_t = \mathbf{x}_t \middle| \sum_{i=1}^n X_{t,i} = n \right] \sum_{i=1}^{N_t} \frac{\binom{x_{t,i}}{k}}{\binom{n}{k}} \mathbb{I}\{x_{t,i} = k\} \\
&= \frac{N_t}{\binom{n}{k}} \sum_{\mathbf{x}_t \in \mathbb{N}_0^{N_t}} \binom{x_{t,1}}{k} \mathbb{P} \left[\mathbf{X}_t = \mathbf{x}_t \middle| \sum_{i=1}^{N_t} X_{t,i} = n \right] \mathbb{I}\{x_{t,1} = k\} \\
&= \frac{N_t}{\binom{n}{k}} \sum_{\mathbf{x}_t^{-(1)} \in \mathbb{N}_0^{N_t-1}} \binom{k}{k} \mathbb{P} \left[X_{t,1} = k, \mathbf{X}_t^{-(1)} = \mathbf{x}_t^{-(1)} \middle| \sum_{i=1}^{N_t} X_{t,i} = n \right] \\
&= \frac{N_t}{\binom{n}{k}} \mathbb{P}[X_{t,1} = k \middle| \sum_{i=1}^{N_t} X_{t,i} = n] \underbrace{\sum_{\mathbf{x}_t^{-(1)} \in \mathbb{N}_0^{N_t-1}} \mathbb{P} \left[\mathbf{X}_t^{-(1)} = \mathbf{x}_t^{-(1)} \middle| \sum_{i=1}^{N_t} X_{t,i} = n, X_{t,1} = k \right]}_{=1} \\
&= \frac{N_t}{\binom{n}{k}} \mathbb{P} \left[X_{t,1} = k \middle| \sum_{i=1}^{N_t} X_{t,i} = n \right]. \tag{5}
\end{aligned}$$

73 Note that $X_{t,i}$ does not follow the same offspring distribution as $S_{t,i}$. $(X_{t,1}, \dots, X_{t,N_t})$ consists of n
 74 individuals sampled from generation $t+1$ without replacement - there is no guarantee that all offspring
 75 from any given parent are included in the sample.

76 **2.3 Complementarity of exclusive coalescence probabilities**

77 If we consider one of the lines observed amongst a set of n , it can either remain uncoalesced (with
 78 probability $p_{n,1,t}$) or coalesce in an event of size k (with probability $p_{n,k,t}$) with any set of $k-1$ lines
 79 among the $n-1$ other lines, leading to the following complementarity equation:

$$\sum_{k=1}^n \binom{n-1}{k-1} p_{n,k,t} = 1 \tag{6}$$

80 We can show that it is indeed satisfied by the formula in Equation (5):

$$\begin{aligned}
\sum_{k=1}^n \binom{n-1}{k-1} p_{n,k,t} &= \sum_{k=1}^n \binom{n-1}{k-1} \frac{N_t}{\binom{n}{k}} \mathbb{P} \left[X_1 = k \mid \sum_{i=1}^{N_t} X_i = n \right] \\
&= \sum_{k=1}^n N_t \frac{k}{n} \mathbb{P} \left[X_1 = k \mid \sum_{i=1}^{N_t} X_i = n \right] \\
&= \frac{N_t}{n} \sum_{k=0}^n k \mathbb{P} \left[X_1 = k \mid \sum_{i=1}^{N_t} X_i = n \right] \\
&= \frac{N_t}{n} \mathbb{E} \left[X_1 \mid \sum_{i=1}^{N_t} X_i = n \right] \\
&= \frac{1}{n} \sum_{i=1}^{N_t} \mathbb{E} \left[X_i \mid \sum_{i=1}^{N_t} X_i = n \right] \\
&= \frac{1}{n} \mathbb{E} \left[\sum_{i=1}^{N_t} X_i \mid \sum_{i=1}^{N_t} X_i = n \right] \\
&= 1
\end{aligned} \tag{7}$$

81 3 Poisson case

82 Here the offspring distribution is $\alpha_t = \text{Poisson}(R_t)$. In this case, we have

$$\sum_{i=1}^{N_t} S_{t,i} \sim \text{Poisson}(N_t R_t), \tag{8}$$

83 and conditional distribution

$$\begin{aligned}
\mathbb{P} \left[S_{t,1} = s \mid \sum_{i=1}^{N_t} S_{t,i} = N_{t+1} \right] &= \frac{\mathbb{P} \left[S_{t,1} = s, \sum_{i=1}^{N_t} S_{t,i} = N_{t+1} \right]}{\mathbb{P} \left[\sum_{i=1}^{N_t} S_{t,i} = N_{t+1} \right]} \\
&= \frac{\alpha_t(s) \mathbb{P} \left[\sum_{i=2}^{N_t} S_{t,i} = N_{t+1} - s \right]}{\mathbb{P} \left[\sum_{i=1}^{N_t} S_{t,i} = N_{t+1} \right]} \\
&= \frac{\frac{R_t^s e^{-R_t}}{s!} \cdot \frac{((N_t - 1)R_t)^{N_{t+1} - s}}{(N_{t+1} - s)!}}{\frac{(N_t R_t)^{N_{t+1}} e^{-N_t R_t}}{N_{t+1}!}} \\
&= \binom{N_{t+1}}{s} \left(\frac{1}{N_t} \right)^s \left(1 - \frac{1}{N_t} \right)^{N_{t+1} - s},
\end{aligned} \tag{9}$$

84 that is

$$S_{t,1} \left| \left(\sum_{i=1}^{N_t} S_{t,i} = N_{t+1} \right) \right. \sim \text{Binomial} \left(N_{t+1}, \frac{1}{N_t} \right). \quad (10)$$

85 The falling factorial moments of $X \sim \text{Binomial}(n, p)$ are (Potts 1953):

$$\mathbb{E} \left[\frac{X!}{(X-r)!} \right] = \binom{n}{r} p^r r! \quad (11)$$

86 By injecting this formula into Equation (3) we obtain the inclusive probability of coalescence for k
87 lines:

$$\mathbb{E} \left[\binom{S_{t,1}}{k} \left| \sum_{i=1}^{N_t} S_{t,i} = N_{t+1} \right. \right] = \frac{1}{k!} \mathbb{E} \left[\frac{S_{t,1}!}{(S_{t,1}-k)!} \left| \sum_{i=1}^{N_t} S_{t,i} = N_{t+1} \right. \right] = \frac{1}{k!} \frac{N_{t+1}!}{(N_{t+1}-k)!} \left(\frac{1}{N_t} \right)^k. \quad (12)$$

88 Consequently, the inclusive probability of coalescence for k lines is

$$p_{k,t} = \frac{1}{N_t^{k-1}}. \quad (13)$$

89 By injecting the probability mass function of a binomial distribution in Equation (5) we deduce that
90 the exclusive probability of coalescence for k lines from a sample of n ($n \geq k$) is

$$p_{n,k,t} = \frac{(N_t - 1)^{n-k}}{N_t^{n-1}}. \quad (14)$$

91 It is interesting to note that neither the inclusive nor the exclusive coalescence probability depend on
92 the mean R_t of the Poisson offspring distribution or the size N_{t+1} of the population at time $t+1$. The
93 inclusive coalescent probability in Equation (13) can also be obtained conceptually by considering that
94 among the k lines, the first one has an ancestor with probability one, and the remaining $k-1$ need
95 to have the same ancestor among a set of N_t from which they choose uniformly at random so that
96 the probability of picking the same ancestor is $1/N_t$. The exclusive coalescent probability in Equation
97 (14) can be derived likewise by considering that in addition to the above, each of the $n-k$ other lines
98 need to choose a different ancestor, which happens with probability $(N_t - 1)/N_t$.

99 Figure 1 illustrates the inclusive and exclusive coalescence probabilities for the Poisson case for a set
100 of size $k = 1$ to $k = 10$ amongst a total of $n = 10$ observed lines, in a population of size $N_t = 10$,
101 $N_t = 20$ or $N_t = 30$.

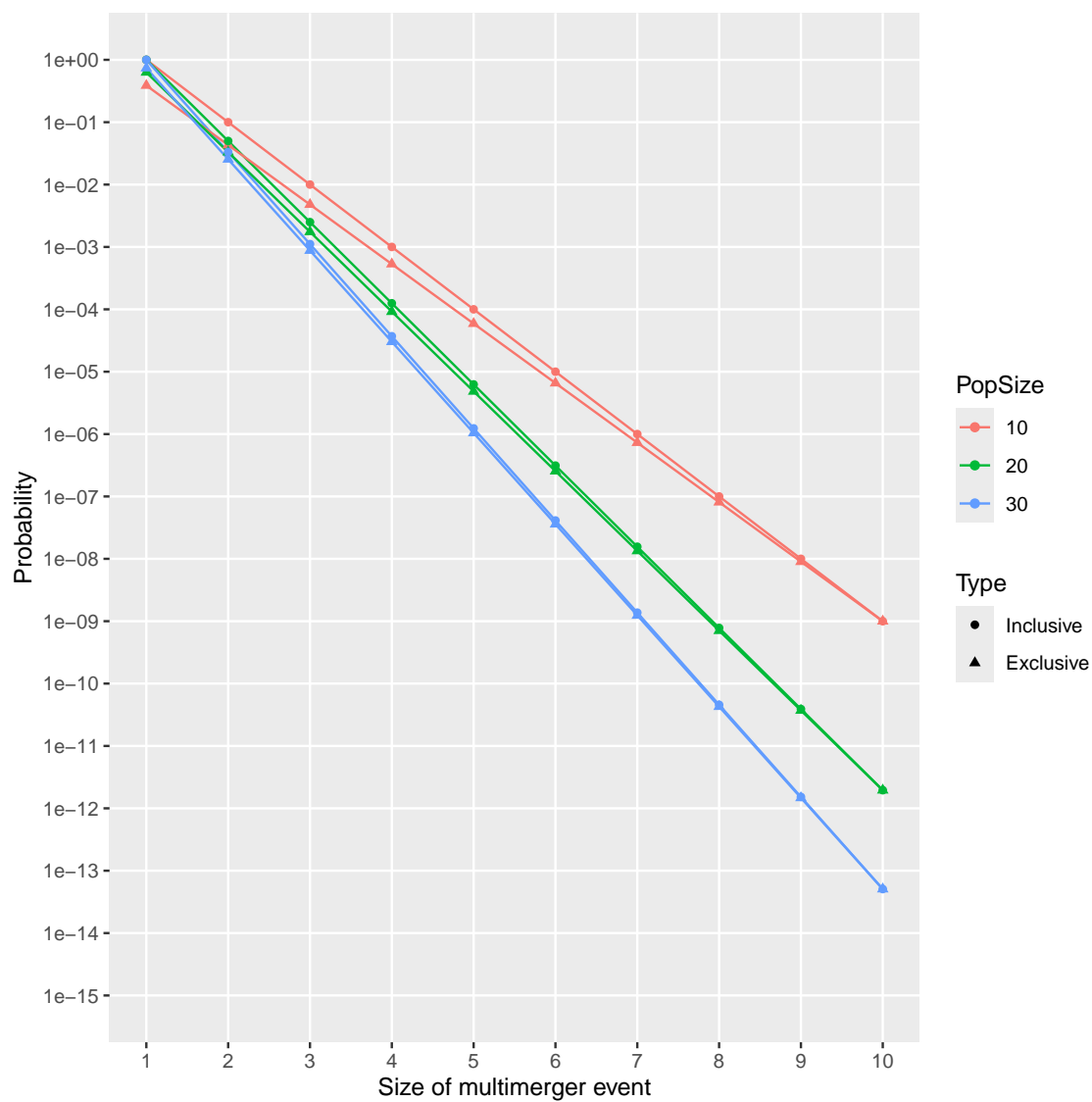


Figure 1: Inclusive and exclusive coalescence probabilities for the Poisson case.

4 Negative-Binomial case

Here the offspring distribution is $\alpha_t = \text{Negative-Binomial}(r, p)$ with parameters (r, p) set my moment-matching mean R_t and variance V_t . The resulting parameters for this distribution are $r = R_t^2/(V_t - R_t)$ and $p = R_t/V_t$. In this case, we have

$$\sum_{i=1}^{N_t} S_{t,i} \sim \text{Negative-Binomial}(N_t r, p), \quad (15)$$

and similarly to the $\text{Poisson}(\lambda)$ offspring distribution identify the conditional distribution of $S_{t,1} | \sum_{i=1}^{N_t} S_{t,i}$ as follows,

$$\begin{aligned} \mathbb{P}\left[S_{t,1} = s \mid \sum_{i=1}^{N_t} S_{t,i} = N_{t+1}\right] &= \frac{\alpha_t(s) \cdot \mathbb{P}\left[\sum_{i=2}^{N_t} S_{t,i} = N_{t+1} - s\right]}{\mathbb{P}\left[\sum_{i=1}^{N_t} S_{t,i} = N_{t+1}\right]} \\ &= \frac{\frac{\Gamma(r+s)}{s!\Gamma(r)}(1-p)^s p^r \cdot \frac{\Gamma((N_t-1)r + (N_{t+1}-s))}{(N_{t+1}-s)!\Gamma((N_t-1)r)}(1-p)^{N_{t+1}-s} p^{(N_t-1)r}}{\frac{\Gamma(N_t r + N_{t+1})}{N_{t+1}!\Gamma(N_t r)}(1-p)^{N_{t+1}} p^{N_t r}} \\ &= \frac{N_{t+1}!}{s!(N_{t+1}-s)!} \frac{\Gamma(r+s)\Gamma((N_t-1)r + (N_{t+1}-s))}{\Gamma(N_t r + N_{t+1})} \frac{\Gamma(N_t r)}{\Gamma(r)\Gamma((N_t-1)r)} \\ &= \binom{N_{t+1}}{s} \frac{B(s+r, N_{t+1}-s + (N_t-1)r)}{B(r, (N_t-1)r)}, \end{aligned} \quad (16)$$

that is

$$S_{t,1} \mid \left(\sum_{i=1}^{N_t} S_{t,i} = N_{t+1}\right) \sim \text{Beta-Binomial}(r, (N_t-1)r). \quad (17)$$

The falling factorial moments of $X \sim \text{Beta-Binomial}(\alpha, \beta)$ are (Tripathi et al. 1994):

$$\mathbb{E}\left[\frac{X!}{(X-r)!}\right] = \binom{n}{r} \frac{B(\alpha+r, \beta)r!}{B(\alpha, \beta)} \quad (18)$$

where $B(x, y)$ denotes the Beta function defined as $B(x, y) = \Gamma(x)\Gamma(y)/\Gamma(x+y)$, and injecting this formula into Equation (3), we deduce that the inclusive probability of coalescence for k lines is:

$$p_{k,t} = \frac{B(N_t r + 1, r + k)}{B(r + 1, N_t r + k)} \quad (19)$$

By injecting the probability mass function of a beta-binomial distribution in Equation (5) we deduce that the exclusive probability of coalescence for k lines is:

$$p_{n,k,t} = \frac{N_t B(k+r, n-k+N_t r-r)}{B(r, N_t r-r)} \quad (20)$$

It is interesting to note that as for the Poisson case, the inclusive and exclusive coalescence probabilities do not depend on the size N_{t+1} of the population at time $t+1$. They both depend on the Negative-Binomial offspring distribution only through the dispersion parameter r .

Figure 2 illustrates the inclusive and exclusive coalescence probabilities for the Negative-Binomial case for a set of size $k = 1$ to $k = 10$ amongst a total of $n = 10$ observed lines, in a population of size $N_t = 12$. Several Negative-Binomial offspring distributions are compared, all of which have the same mean $R_t = 2$, and with the dispersion parameter equal to $r = 1$, $r = 2$, $r = 10$ and $r = 100$. When $r = 1$ the Negative-Binomial reduces to a Geometric distribution. When r is high (for example $r = 100$ as shown in Figure 2) the dispersion is low and the Negative-Binomial case behaves almost like the Poisson case. When r is lower the dispersion of the offspring distribution increases, so that both the inclusive and exclusive probabilities of larger multimerger events increase.

5 Limit when the population size is large

Consider that N_t is large.

Show that inclusive probabilities $p_{k,t}$ for $k > 2$ are small compared to $p_{2,t}$.

Show that exclusive probabilities $p_{n,k,t}$ for $k > 2$ is small compared to $p_{n,2,t}$, when $n \ll N_t$.

Show that inclusive and exclusive probabilities become equal, when $n \ll N_t$ in exclusive probabilities.

For Poisson offspring distribution we have:

$$p_{2,t} = p_{n,2,t} = \frac{1}{N_t} \quad (21)$$

For Negative-Binomial offspring distribution we have:

$$p_{2,t} = p_{n,2,t} = \frac{r+1}{N_t r + 1} \approx \frac{r+1}{N_t r} \quad (22)$$

Fraser and Li (2017) calculated the effective population size $N_e(t)$ as a function of the actual population size $N(t)$ and the mean and variance of the offspring distribution R and σ^2 :

$$N_e(t) = \frac{N(t)}{\sigma^2/R + R - 1} \quad (23)$$

This formula was used to estimate the dispersion parameter from genetic data (Li et al. 2017). In our notation, this is equivalent to:

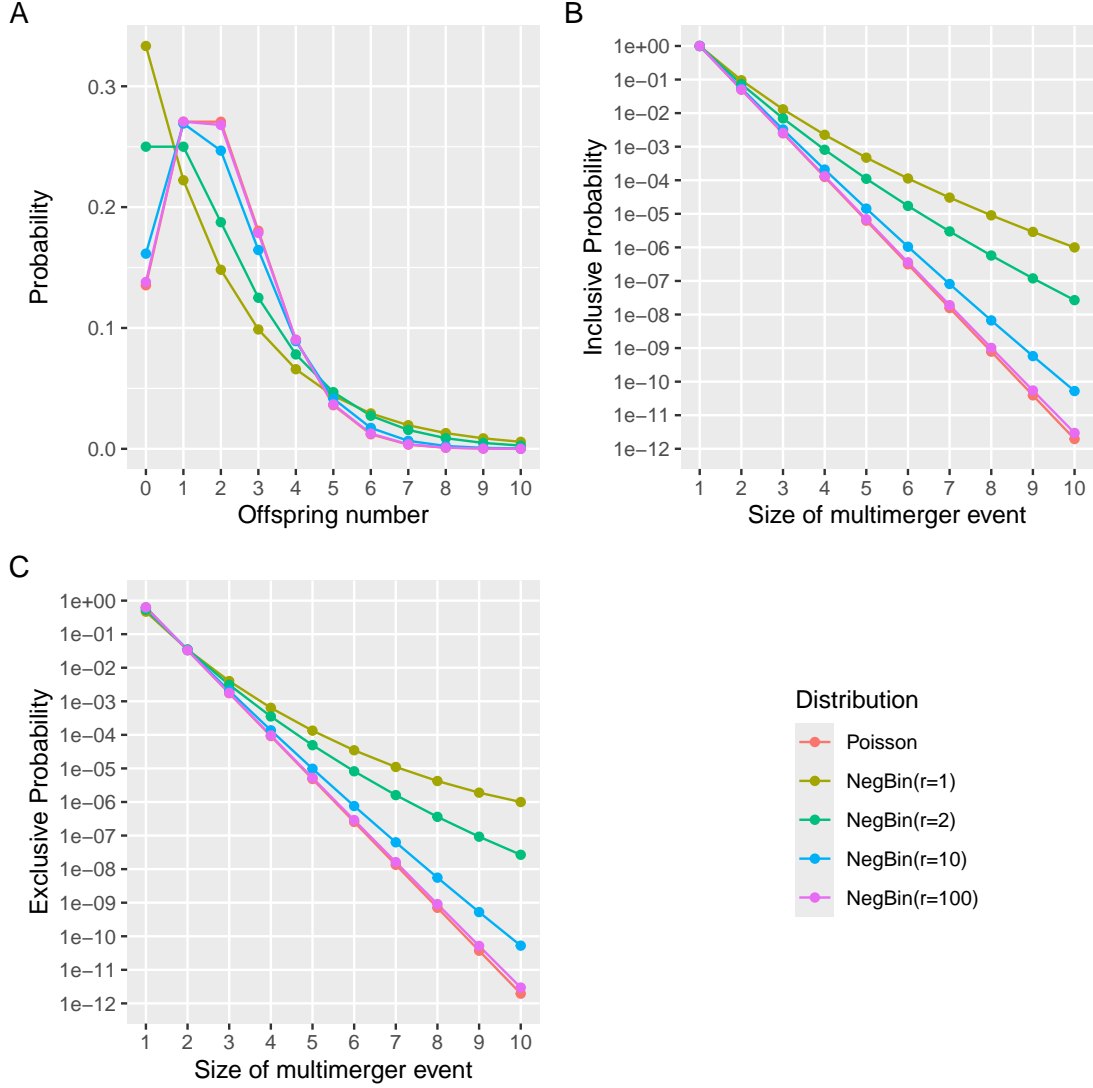


Figure 2: (A) Offspring distribution. (B) Inclusive probability of coalescence. (C) Exclusive probability of coalescence.

$$p_{2,t} = \frac{V_t/R_t + R_t - 1}{N_t R_t} \quad (24)$$

136 In the Poisson case we have $V_t = R_t$ so that Equation (24) simplifies to $p_{2,t} = 1/N_t$ which agrees with
 137 Equation (21). In the Negative-Binomial case we have $V_t/R_t = 1/p = (r + R_t)/r$ so that Equation
 138 (24) simplifies to $(r + 1)/(rN_t)$ which agrees with our Equation (22). Conversely, if we substitute
 139 $r = R_t^2/(V_t - R_t)$ in Equation (22) we obtain the formula Equation (24).

140 Koelle and Rasmussen (2012) derived the rates of coalescence of two lineages for several epidemiological

models, assuming a large population at equilibrium. For each model they use the equation $N_e = N/\sigma^2$ to relate the effective population size N_e to the actual population size N and the variance σ^2 in the number of offspring. This relationship was first established by Kingman (1982a) to apply the coalescent model to Cannings exchangeable models (Cannings 1974). From Equation (22) we can take $R_t = 1$ to achieve equilibrium of the population size and $r = R_t^2/(V_t - R_t) = 1/(V_t - 1)$ to deduce the equivalent $p_{2,t} = V_t/N_t$.

Volz (2012) showed that the rate of coalescence for two lineages under a continuous-time epidemic coalescent model is $2f(t)/I(t)^2$ where $f(t)$ is the incidence and $I(t)$ the prevalence. Setting in this formula the prevalence as $I(t) = N_{t+1} = N_t R_t$ and the incidence as $f(t) = R_t N_{t+1} = R_t^2 N_t$ we get a coalescent rate of $2/N_t$. To apply the Equation (22) we need to set $r = 1$ so that the offspring distribution is Geometric, which yields the same result.

6 Lambda-coalescent

The coalescent model (Kingman 1982a,b) describes the ancestry of a sample from a large population evolving according to many forward-in-time models such as the Wright-Fisher model (Wright 1931; Fisher 1930), the Moran model (Moran 1958) and the Cannings exchangeable model (Cannings 1974). Since the coalescent considers a large population in which each individual only has a number of offspring that is small compared to the population size, coalescent trees are always binary and do not feature multimergers, making them unsuitable to represent the ancestry of outbreaks considered in this study. However, the lambda-coalescent models are an extension of the coalescent model that do allow multimergers (Pitman 1999; Sagitov 1999; Donnelly and Kurtz 1999).

A lambda-coalescent model is defined by a probability measure $\Lambda(dx)$ on the interval $[0, 1]$, from which we can deduce the rate $\lambda_{n,k}$ at which any subset of k lineages within a set of n observed lineages coalesce:

$$\lambda_{n,k} = \int_0^1 x^{k-2} (1-x)^{n-k} \Lambda(dx) \quad (25)$$

The beta-coalescent (Schweinsberg 2003) is a specific type of lambda-coalescent. Was used in (Hoscheit and Pybus 2019) and (Menardo et al. 2021). David's paper on inference of multiple mergers while dating a pathogen phylogeny (Helekal et al. 2024). The Beta($2 - \alpha, \alpha$)-coalescent model has a single parameter $\alpha \in [0, 2]$ and is defined as:

$$\Lambda(dx) = \frac{x^{1-\alpha} (1-x)^{\alpha-1}}{B(2-\alpha, \alpha)} dx \quad (26)$$

from which we can deduce that:

$$\lambda_{n,k} = \frac{B(k-\alpha, n-k+\alpha)}{B(2-\alpha, \alpha)} \quad (27)$$

169 Special cases of the beta-coalescent include $\alpha = 2$ corresponding to the Kingman coalescent, $\alpha = 1$
 170 which is known as the Bolthausen-Sznitman coalescent and $\alpha = 0$ for which the phylogeny is always
 171 star-shaped.

172 We now define our own lambda-coalescent based on the Negative-Binomial case describe previously.
 173 The ease of comparison with other coalescent models, we consider that time is continuous, and that
 174 the population size remains fixed at N_t . The exclusive coalescent probability $p_{n,k,t}$ in the Negative-
 175 Binomial case given by Equation (20) can be used to determine the corresponding rate of our lambda-
 176 coalescent:

$$\lambda_{n,k} = -\log(1 - p_{n,k,t}) \quad (28)$$

177 In order to compare our lambda-coalescent with other models, we consider the distribution of the size
 178 k of the next event among a set of n lineages. For any lambda-coalescent this can be computed as:

$$p(k|n) = \frac{\binom{n}{k} \lambda_{n,k}}{\sum_{i=2}^n \binom{n}{i} \lambda_{n,i}} \quad (29)$$

179 Figure 3 compares this distribution for $n = 10$ in the Beta-coalescent with parameter $\alpha \in \{0.5, 1, 1.5\}$
 180 and for our lambda-coalescent with parameters $N_t \in \{15, 25, 50\}$ and $r \in \{0.1, 0.5, 1\}$.

181 Figure 4 shows examples of trees simulated for a sample of size $n = 20$ and with constant population
 182 size $N_t = 40$.

183 Figure 5 shows summary statistics for 10,000 trees simulated in the same conditions as the individual
 184 trees shown in Figure 4. As the dispersion parameter increases from $r = 0.1$ to $r = 10$ multimerger
 185 events become less and less likely and large. Simultaneously, the time to the most recent common
 186 ancestor increases, as well as the stemminess of the tree (ie the proportion of branch lengths in non-
 187 terminal branches).

188 7 Implementation

189 We implemented the analytical methods described in this paper in a new R package entitled *EpiLambda*
 190 which is available at <https://github.com/xavierdidelot/EpiLambda> for R version 3.5 or later. All
 191 code and data needed to replicate the results are included in the “run” directory of the *EpiLambda*
 192 repository.

193 8 Discussion

194 Our lambda-coalescent could be defined in a varying population size and/or with temporally offset
 195 leaves following the same approach as previously described for the beta-coalescent (Hoscheit and Pybus
 196 2019).

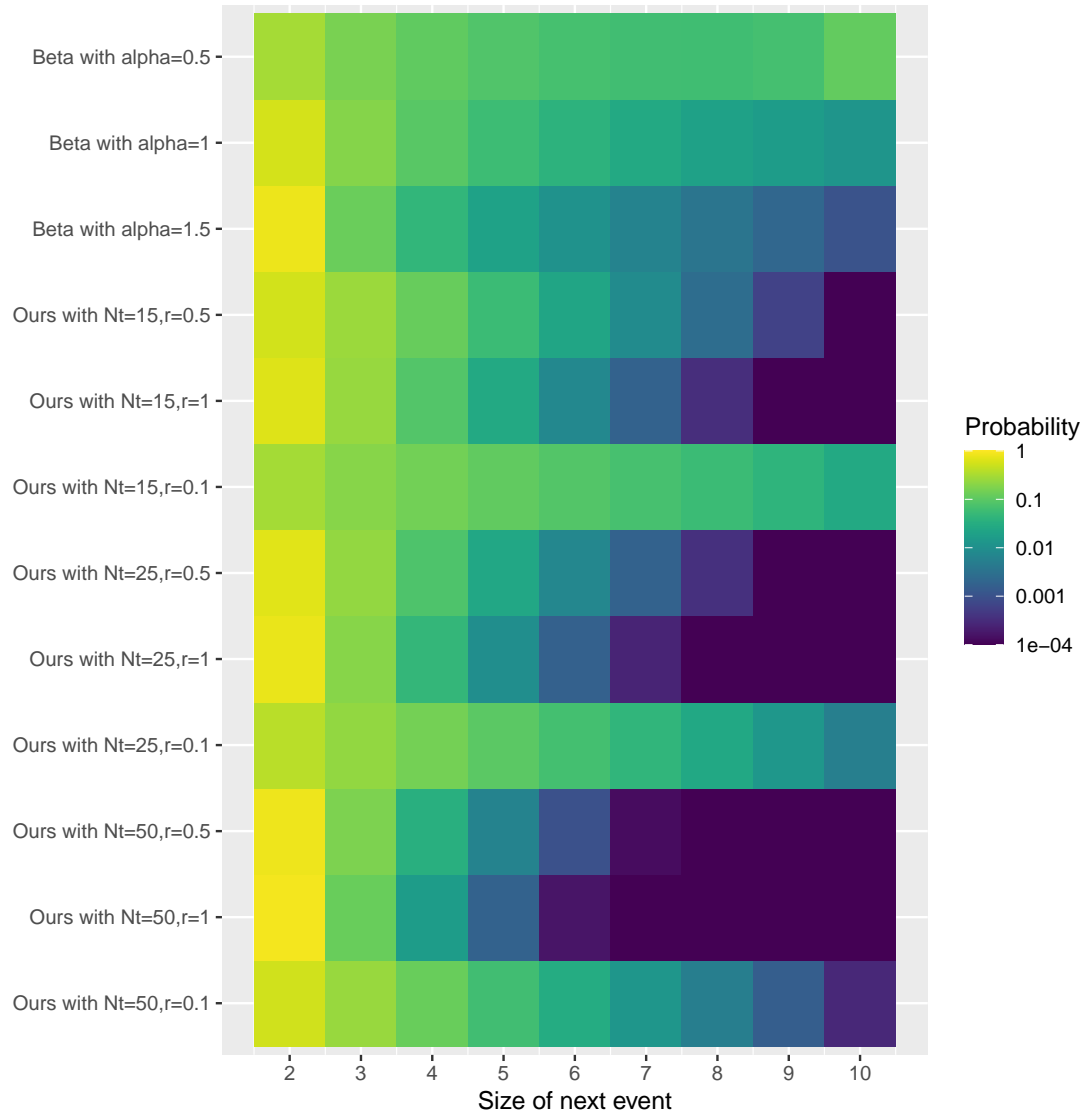


Figure 3: Distribution of the size of the next event among a set of $n = 10$ lineages, compared between the Beta-coalescent and our lambda-coalescent model with various parameters.

197 Either here or before discuss the Xi-coalescent models which admit multiple simultaneous mergers
 198 (Schweinsberg 2000).

199 Acknowledgements

200 We acknowledge funding from the National Institute for Health Research (NIHR) Health Protection
 201 Research Unit in Genomics and Enabling Data.

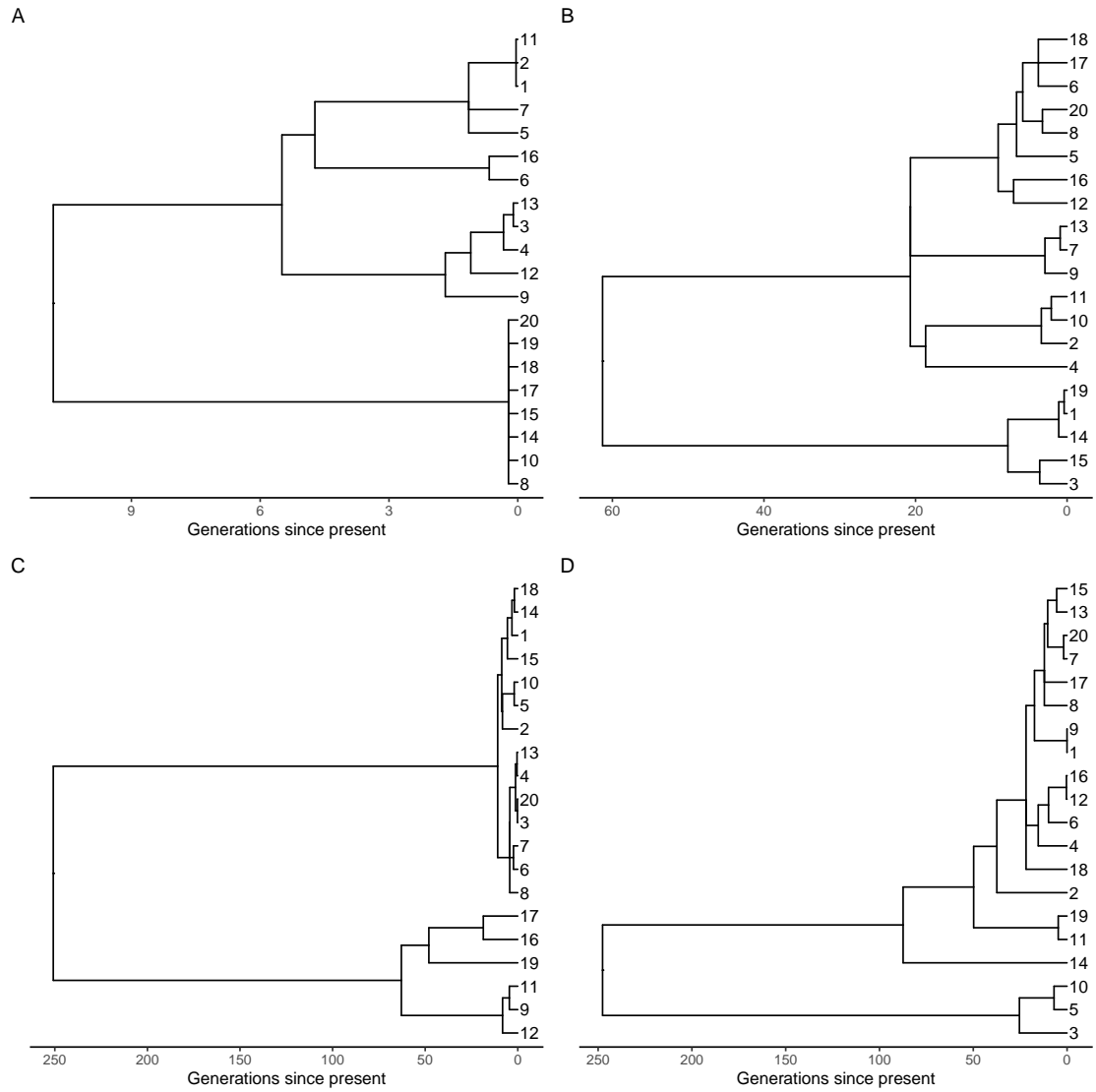


Figure 4: Example of trees simulated under our lambda-coalescent with $r = 0.1$ (A), $r = 1$ (B), $r = 5$ (C) and $r = 10$ (D).

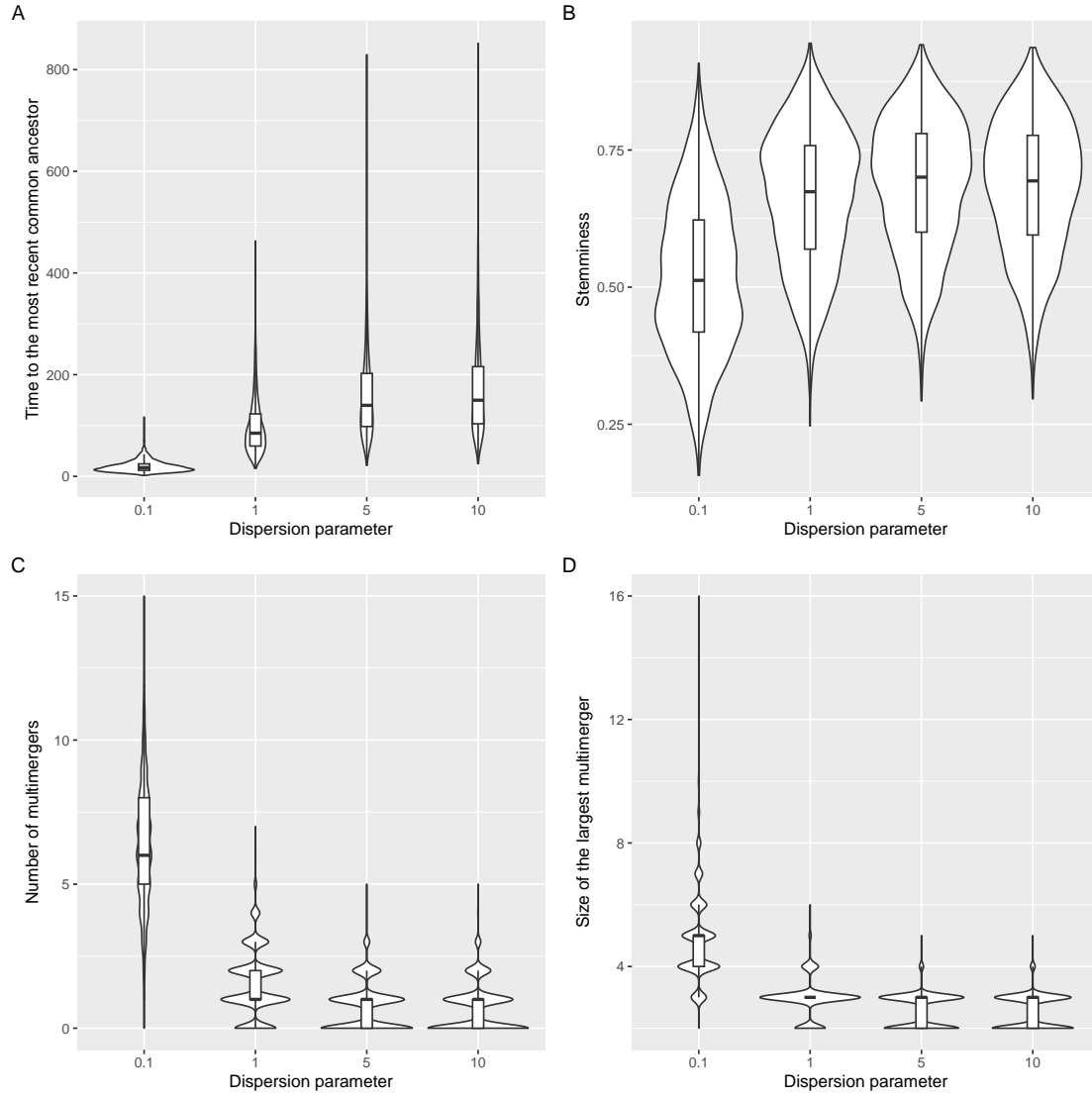


Figure 5: Summary statistics for trees simulated under our lambda-coalescent with $r = 0.1, r = 1, r = 5$ and $r = 10$, namely the time to the most recent common ancestor (A), stemminess (B), number of multimerers (C) and the size of the largest multimerger (D).

References

- Anderson, R.M., May, R.M., 1991. Infectious Diseases of Humans: Dynamics and Control. Oxford University Press, USA.
- Cannings, C., 1974. The latent roots of certain Markov chains arising in genetics: a new approach, I. Haploid models. *Adv. Appl. Probab.* 6, 260–290. doi:10.2307/1426293.
- Donnelly, P., Kurtz, T.G., 1999. Particle Representations for Measure-Valued Population Models. *The Annals of Probability* 27. doi:10.1214/aop/1022677258.
- Fisher, R.A., 1930. The genetical theory of natural selection. Clarendon Press. doi:10.5962/bh1.title.27468.
- Fraser, C., Li, L.M., 2017. Coalescent models for populations with time-varying population sizes and arbitrary offspring distributions. *bioRxiv* , 10.1101/131730doi:10.1101/131730.
- Fraser, C., Riley, S., Anderson, R.M., Ferguson, N.M., 2004. Factors that make an infectious disease outbreak controllable. *Proceedings of the National Academy of Sciences* 101, 6146–6151. doi:10.1073/pnas.0307506101.
- Gómez-Carballa, A., Pardo-Seco, J., Bello, X., Martínón-Torres, F., Salas, A., 2021. Superspreading in the emergence of COVID-19 variants. *Trends in Genetics* 37, 1069–1080. doi:10.1016/j.tig.2021.09.003.
- Grassly, N.C., Fraser, C., 2008. Mathematical models of infectious disease transmission. *Nature Reviews Microbiology* 6, 477–87. doi:10.1038/nrmicro1845.
- Helekal, D., Koskela, J., Didelot, X., 2024. Inference of multiple mergers while dating a pathogen phylogeny. *bioRxiv* , 2023.09.12.557403doi:10.1101/2023.09.12.557403.
- Hoscheit, P., Pybus, O.G., 2019. The multifurcating skyline plot. *Virus Evolution* 5, 1–10. doi:10.1093/ve/vez031.
- Keeling, M.J., Rohani, P., 2008. Modeling infectious diseases in humans and animals. Princeton university press.
- Kingman, J., 1982a. The coalescent. *Stochastic Processes and their Applications* 13, 235–248. doi:10.1016/0304-4149(82)90011-4.
- Kingman, J.F.C., 1982b. On the genealogy of large populations. *Journal of Applied Probability* 19, 27–43. doi:10.2307/3213548.
- Koelle, K., Rasmussen, D.A., 2012. Rates of coalescence for common epidemiological models at equilibrium. *Journal of The Royal Society Interface* 9, 997–1007. doi:10.1098/rsif.2011.0495.
- Lemieux, J.E., Siddle, K.J., Shaw, B.M., Loreth, C., Schaffner, S.F., Gladden-Young, A., Adams, G., Fink, T., Tomkins-Tinch, C.H., Krasilnikova, L.A., DeRuff, K.C., Rudy, M., Bauer, M.R., Lagerborg, K.A., Normandin, E., Chapman, S.B., Reilly, S.K., Anahtar, M.N., Lin, A.E., Carter, A., Myhrvold, C., Kembell, M.E., Chaluvadi, S., Cusick, C., Flowers, K., Neumann, A., Cerrato, F., Farhat, M., Slater, D., Harris, J.B., Branda, J.A., Hooper, D., Gaeta, J.M., Baggett, T.P., O’Connell, J., Gnirke, A., Lieberman, T.D., Philippakis, A., Burns, M., Brown, C.M., Luban, J., Ryan, E.T., Turbett, S.E., LaRocque, R.C., Hanage, W.P., Gallagher, G.R., Madoff, L.C., Smole, S., Pierce, V.M., Rosenberg, E., Sabeti, P.C., Park, D.J., MacInnis, B.L., 2021. Phylogenetic analysis of SARS-CoV-2 in Boston highlights the impact of superspreading events. *Science* 371, eabe3261. doi:10.1126/science.abe3261.

Li, L.M., Grassly, N.C., Fraser, C., 2017. Quantifying Transmission Heterogeneity Using Both Pathogen Phylogenies and Incidence Time Series. *Molecular Biology and Evolution* 34, 2982–2995. doi:10.1093/molbev/msx195.

Lloyd-Smith, J., Schreiber, S., Kopp, P., Getz, W., 2005. Superspreading and the effect of individual variation on disease emergence. *Nature* 438, 355–9. doi:10.1038/nature04153.

Menardo, F., Gagneux, S., Freund, F., 2021. Multiple Merger Genealogies in Outbreaks of *Mycobacterium tuberculosis*. *Molecular Biology and Evolution* 38, 290–306. doi:10.1093/molbev/msaa179.

Moran, P., 1958. Random Processes in Genetics. *Mathematical Proceedings of the Cambridge Philosophical Society* 54, 60–71.

Pitman, J., 1999. Coalescents with multiple collisions. *The Annals of Probability* 27, 1870–1902.

Potts, R.B., 1953. Note on the Factorial Moments of Standard Distributions. *Australian Journal of Physics* 6, 498–499. URL: <https://www.publish.csiro.au/ph/ph530498>, doi:10.1071/ph530498. publisher: CSIRO PUBLISHING.

Sagitov, S., 1999. The general coalescent with asynchronous mergers of ancestral lines. *Journal of Applied Probability* 36, 1116–1125. doi:10.1239/jap/1032374759.

Schweinsberg, J., 2000. Coalescents with Simultaneous Multiple Collisions. *Electronic Journal of Probability* 5. doi:10.1214/EJP.v5-68.

Schweinsberg, J., 2003. Coalescent processes obtained from supercritical Galton–Watson processes. *Stochastic Processes and their Applications* 106, 107–139. doi:10.1016/S0304-4149(03)00028-0.

Stein, R.A., 2011. Super-spreaders in infectious diseases. *International Journal of Infectious Diseases* 15, e510–e513. doi:10.1016/j.ijid.2010.06.020.

Tripathi, R.C., Gupta, R.C., Gurland, J., 1994. Estimation of parameters in the beta binomial model. *Annals of the Institute of Statistical Mathematics* 46, 317–331. URL: <https://doi.org/10.1007/BF01720588>, doi:10.1007/BF01720588.

Volz, E.M., 2012. Complex population dynamics and the coalescent under neutrality. *Genetics* 190, 187–201. doi:10.1534/genetics.111.134627.

Wang, J., Chen, X., Guo, Z., Zhao, S., Huang, Z., Zhuang, Z., Wong, E.L.y., Zee, B.C.Y., Chong, M.K.C., Wang, M.H., Yeoh, E.K., 2021. Superspreading and heterogeneity in transmission of SARS, MERS, and COVID-19: A systematic review. *Computational and Structural Biotechnology Journal* 19, 5039–5046. doi:10.1016/j.csbj.2021.08.045.

Wang, L., Didelot, X., Yang, J., Wong, G., Shi, Y., Liu, W., Gao, G.F., Bi, Y., 2020. Inference of person-to-person transmission of COVID-19 reveals hidden super-spreading events during the early outbreak phase. *Nature Communications* 11, 5006. doi:10.1038/s41467-020-18836-4.

Woolhouse, M.E.J., Dye, C., Etard, J.F., Smith, T., Charlwood, J.D., Garnett, G.P., Hagan, P., Hii, J.L.K., Ndhlovu, P.D., Quinnell, R.J., Watts, C.H., Chandiwana, S.K., Anderson, R.M., 1997. Heterogeneities in the transmission of infectious agents: Implications for the design of control programs. *Proceedings of the National Academy of Sciences* 94, 338–342. doi:10.1073/pnas.94.1.338.

Wright, S., 1931. Evolution in Mendelian populations. *Genetics* 16, 97–159. doi:10.1093/genetics/16.2.97.